An analytical approach to error detection and correction for onboard nanosatellites

Md. Motaharul Islam[1]* , Mahmudul Hasan[1] and Zaheed Ahmed Bhuiyan[1]

*Correspondence:
motaharul@cse.uiu.ac.bd

[1] Department of Computer Science and Engineering, United International University, United City, Dhaka, Bangladesh

Abstract

Nanosatellites are persistently progressing and creating global communication and data transmission. It builds up a colossal request for more progressed and dependable frameworks to transmit faster and more reliable information. A syntactic machine learning approach has been distinguished as a good plot for anticipating single-bit and multiple-bit errors that influence onboard nanosatellites. In this paper, we have proposed an analytical approach to error detection and correction for onboard nanosatellites. We have planned the framework separately with three distinct parts: encoding, error checking, and decoding. It has created an amid information exchange from satellite to the ground station. It has analyzed six camera pictures simultaneously with the assistance of field programmable gate array and EDAC strategies. We have presented the progressed turbo mechanics EDAC for unprecedented transfer speeds of satellite communication and execution & examination with the AWGN and Rayleigh channels to extend the proficiency. EDAC strategies codes have been implemented in MATLAB. This method is straightforward and accomplishes unwavering quality and exactness compared to comparable strategies.

Keywords: Error detection and correction, Low-density parity check, Bose–Chaudhuri–Hocquenghem codes, Turbo codes, Convolutional codes, Shannon's theorem, Earth observation, Field programmable gate array, On-board command data handling

1 Introduction

A nanosatellite is a device that moves in an elliptical way around a planet. Earth observation (EO) satellite is one of the fundamental devices for investigating the environment [1]. EO satellites apply high-resolution image sensors from the earth's surface to watch and get data. It utilizes infrared for underneath observation. By watching the ground from space, EO satellites give fundamental data on climate observation, urban and rural development, natural disasters, natural monitoring, etc. [2]. During data transmission usually we miss valuable data due to interference.

 Nanosatellite's error detection and correction devices aim to transmit secured and error-less information between the satellite and the ground station [3]. They are subject to unsteady and unstable data corruption because of thermal noise, high energy particle impact, or other noise [4]. Single-bit and burst errors are common satellite data

Islam *et al. J Wireless Com Network*   (2023) 2023:49

Page 2 of 23

communication errors [5]. A single-bit error implies one bit changed from 0 to 1, and a burst error suggests more than one conjugated bit degraded [6]. The mistake discovery handle is the primary step to error redress, which is subordinate to adding extra bits to the first information [7].

Excess bits are accomplished through two basic coding plans: convolution and block coding. Error correction can be classified as a forward error correction (FEC) and automatic repeat request (ARQ). Sometimes ARQ and FEC can be combined [6]. This strategy is called a hybrid automatic-repeat request program. There are numerous frameworks outlined to distinguish and redress mistakes. We have introduced this core error detection and correction (EDAC) algorithm with low-density parity check (LDPC), Turbo code, Bose Chaudhuri Hocquenghem (BCH) code, Convolutional code, and Shannon's theorem to our system for increasing the proficiency of EDAC. We have also analyzed their combined form. We have presented a progressed turbo component with two interleaved, five encoding and interpreting forms. All the mechanisms have been implemented in MATLAB with additive white Gaussian noise (AWGN) and Rayleigh channel.

The main contributions of this paper are as follows:

- We have proposed an innovative architecture that consists of the EDAC method for the nanosatellites. It has analyzed six camera images simultaneously with the assistance of FPGA.
- We have analyzed, and compared the satellites' error detection and correction algorithms. We have also developed our proposed hybrid approach for EDAC.
- We have identified the number of erroneous bits. Based on that, we have developed a syntactic analysis for the error correction method.
- We have implemented the scheme for the LDPC, BCH, Turbo, Convolutional, and Shannon's theorem. The scheme shows that the BER ratio gradually decreases from 10^{-1} to 10^{-6}; on the other hand, system performance increases significantly.
- We have discussed the limitations of existing error detection and correction algorithms. We have proposed future work to introduce an advanced error detection method based on satellite-transmitted data using machine learning techniques and to implement the ASIC architecture in Spartan 6 FPGA, a novel approach to improving the accuracy and reliability of nanosatellite data transmission systems.
- Finally, we have analyzed the performance of five different EDAC algorithms with AWGN and Rayleigh channels in MATLAB.

The rest of the paper has been organized in the following ways. Section 2 discusses the literature reviews. Section 3 depicts the architecture of the nanosatellite. Section 4 shows the algorithmic investigation and performance analysis of EDAC Mechanism V-1.1. Sections 5 and 6 describe the EDAC Mechanism V-1.2 and EDAC Mechanism V-1.3. Section 7 shows the performance evaluation graphs. Section 8 describes the limitation and future work of EDAC. Finally, Sect. 9 concludes the paper.

Islam *et al. J Wireless Com Network*   (2023) 2023:49

Page 3 of 23

2 Related works

Mamun et al. [1] proposed a Hamming Code to prevent parity and single-bit error onboard satellites in low earth orbit (LEO). The focus is to work on EDAC via generating a Hamming Code matrix [4, 11, 16]. MATLAB is used for the implementation process of both single-bit and double-bit errors. Pakartipangi et al. [8] proposed a technique for obtaining more comprehensive coverage area images for low dimensions satellites. The system handles all the error bits using the XULA2 LX9 field programmable gate array board, and the camera array was designed so that overlapping areas cannot be found. Ahmed Hanafi et al. [9] proposed an SRAM-based FPGA technology that implements an onboard computer system and uses low-earth orbit nanosatellites. The system was designed to develop payload architecture and an inherent space environment. Ibrahim et al. [10] proposed a satellite system designed with acceptable accuracy in a low-power system. This paper presents a concept to establish avionics systems by utilizing crucial features with the available FPGAs. Scrubbing keeps the FPGA data configurations safe with frame calculation and back-tracking methods.

Daniel et al. [11] proposed a technique that describes a guideline for simulating the system's accuracy providing the necessary statistics to support the decision system regarding the necessary methodology to be implemented [11]. The system is designed to monitor air pollution in Mexican and Latin American cities. Wilson at el. [12] proposed two major supervised themes, hybrid computing and reconfigurable computing [12]. The system survey of the imposition and convenience of small satellites also focuses on new technologies, methods and implementation for the next generation [12]. Banu et al. [13] proposed an encryption method to secure terrestrial communication via a small satellite. Increased quantity of sending valuable and sensitive data, a satellite can bring risks of providing access to unauthorized data. An advanced encryption standard method is used to protect data from such threats. Banu et al. [14] proposed a commercial algorithm called Advanced Encryption Standard (AES). To protect sensitive data and prevent unauthorized access in terrestrial communication, 5 modes of AES in satellite imaging have been used. To prevent the fault from noisy channels and the effect of SEUs, the 5 modes were analyzed and observed using Hamming error correction code.

Hiler et al. [2] proposed a parity check matrix and a calculated syndrome of EDAC onboard nanosatellites. The scheme can self-detect and self-correct any single event effect errors during transmission. BENTOUTOU et al. [15] proposed an onboard EDAC method to protect data transmission between the AISAT-1 CPU and its memory. Wang et al. [16] mentioned a comparison of correction codes for correcting colossal burst data ruins. Colossal burst errors happen in communication driving to different chosen bit errors. They compare the CCSDS codes, such as RS codes convolution, turbo, and LDPC codes. Gao et al. [17] give thought to LDPC codes for the joint attendant and characteristic broadcasting framework. In this paper, they highlighted an earthbound broadcasting framework called time broadcasting-wireless which encompasses China and some other parts of Asia. This framework gives excellent execution results, especially for combined deciphering.

3 Methods

Satellite onboard command data handling structures are shown in Fig. 1. For a low-cost framework of the nanosatellite, a single chip executed onboard command data handling (OBCDH) was proposed for a mixed-mode application-specific integrated circuit (ASIC) [9]. Future Nano Satellites, which have information handling and control capacities with information collecting and further detecting capabilities for Soil perception Missions, result from ASIC detail. Square graph Fig. 1 comprises 4 subsystems where a 32-bit RISC processor center is adjusted for space utilization, a subsystem of picture dealing with the unit, a communication association for the satellite, and a supporting fringe subsystem. OBC is the most component of two scaled-down OBCDH frameworks. To serve an introductory model of the advanced portion of the OBCDH ASIC, this onboard computer framework on a chip Fig. 1. Within the OBCDH, our fundamental need is to upgrade the EDAC framework to have error-free information on disciple communication.

In EDAC, mechanisms V-1.1, V-1.2 and V-1.3 describe the different approaches to solving the satellite communication error and analyze the performance of different channels. Different EDAC Mechanisms have different bit error rates (BER). If we combine multiple encoding methods in a single one, the BER will be reduced, and the system's performance will be much higher than the single encoding method. We have proposed an architecture comprising the top 5 EDAC methods for the nanosatellites.
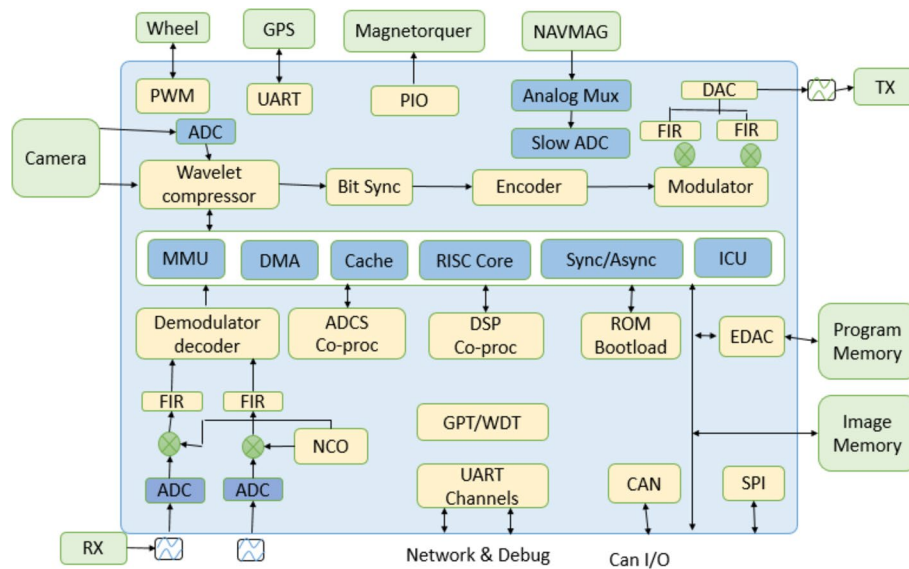

Fig. 1 Satellite OBCHD ASIC structure. Figure comprises 4 subsystems where a 32-bit RISC processor center is adjusted for space utilization, a subsystem of picture dealing with the unit, a communication association for the satellite, and a supporting fringe subsystem. OBC is the most component of two scaled-down OBCDH frameworks. To serve an introductory model of the advanced portion of the OBCDH ASIC, this onboard computer framework on a chip shown in figure
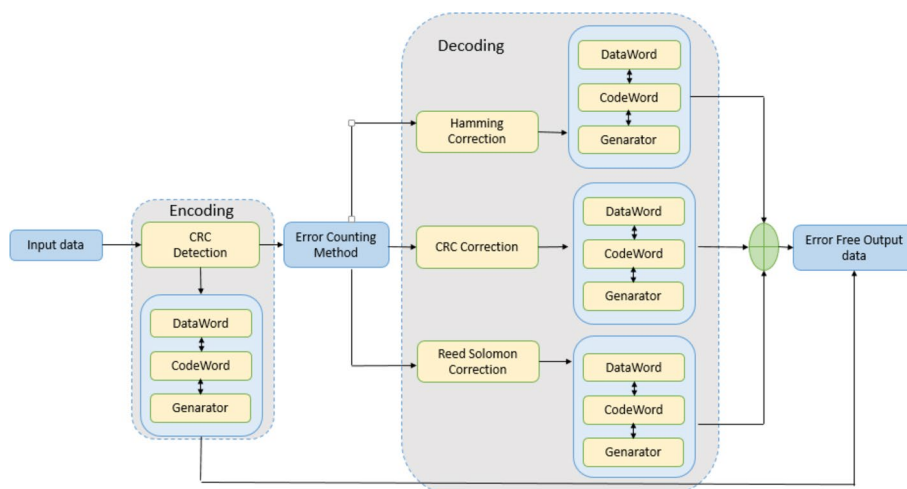
Fig. 2 EDAC proposed algorithmic structure. Nanosatellites that transmit information to the ground station from their blunders be checked with the assistance of a few calculations. Within the ground station, CRC checks blunder information. After that step, with a sort of blunder, able to get the information indicated by detection methods. Within the location strategies, we figure out whether blunders are shown in our data in case of able to distinguish using three steps like information word codeword generator at that point able to recognize the erroneous bit within the input stream appeared in figure

4 EDAC mechanism V-1.1

Nanosatellites that transmit information to the ground station from their blunders be checked with the assistance of a few calculations. Within the ground station, CRC checks blunder information. After that step, with a sort of blunder, able to get the information indicated by detection methods. Within the location strategies, we figure out whether blunders are shown in our data in case of able to distinguish using three steps like information word codeword generator at that point able to recognize the erroneous bit within the input stream appeared in Fig. 2. We ought to alter our calculations based on our mistakes, agreeing to the measure of mistakes. In these adjustment strategies like Hamming, CRC and Reed Solomon codes, we would present our less error information with the assistance of these adjustment strategies.

4.1 Hamming code

Hamming code could be a direct piece code for blunder location and redress. It can identify one-bit or two bits mistakes at the same time and can rectify them as if they were single-bit mistakes. The fundamental concept of the hamming code is to include an equality bit after the stream of information to confirm that the ground station got the information and matches the comparing input information stream. Partisan ground stations check the transmitted information to distinguish where the mistake happened. The structure of the hamming code has a square length, message length, and separation. Square length characterizes as $n = 2r - 1$ where $r > = 2$ message length and remove the inclusion $2r - r - 1$. Depending on the hamming code adaptation, remove the error bit that got changed. It includes more than one error bit, which can find the blunder's position and self-correct it by altering the bit. Generally, three sorts of hamming codes are utilized in Nano-satellite communication as Hamming [3, 4, 7], Hamming [4, 4, 8], and Hamming [4, 11, 16].

Islam *et al. J Wireless Com Network*   (2023) 2023:49

Page 6 of 23

4.2 Cyclic redundancy check

CRC is the method of accepting emerging alter blunders within the communication channel. Satellite information trade is based on CRC codes, and the EDAC process broadly utilized in advanced CRC code is additionally commonly alluded to as polynomial codes -1 on a thin wire. Working on a thin wire is characterized as polynomial checks. The k-bit message is considered a polynomial condition list with the words k, from $x^{(k-1)}$ to x^0. The most noteworthy arrangement is the coefficient of $x^{(k-1)}$, the proportionate of $x^{(k-2)}$, and so on. Test digits are created by rehashing the k-bit message x^n and partly produced by $rm(n+1)$ bits polynomial code. The excite n -bit adjust is passed as test digits. The same polynomial generator separates the total collection grouping. If the remaining pieces are zero, no mistakes have occurred. If the remaining pieces are not zero, an exchange blunder happens.

4.3 Reed Solomon

Reed Solomon codes work with a burst sort of information mistake. It is also used as a broadcast framework in adjustment code communication, capacity framework, etc. [18]. It recognizes the burst blunder of information transmission and amends those blunder information. If the Reed Solomon codes are utilized at that point, the likelihood of an error remaining within the decoded information will be much lower [19]. Reed Solomon codes are too appropriate for different burst blunder adjustment codes as a grouping of $b+1$ sequential mistakes can influence up to 2 signals of measure excite b [20]. The exciting alternative goes to the coding architect and can be chosen over a wide range.

Reed Solomon's mistake adjustment may be a forward-looking blunder code [21]. It works with polynomial tests of information. Polynomials have been tried in a few places, and these numbers are either transmitted or recorded.
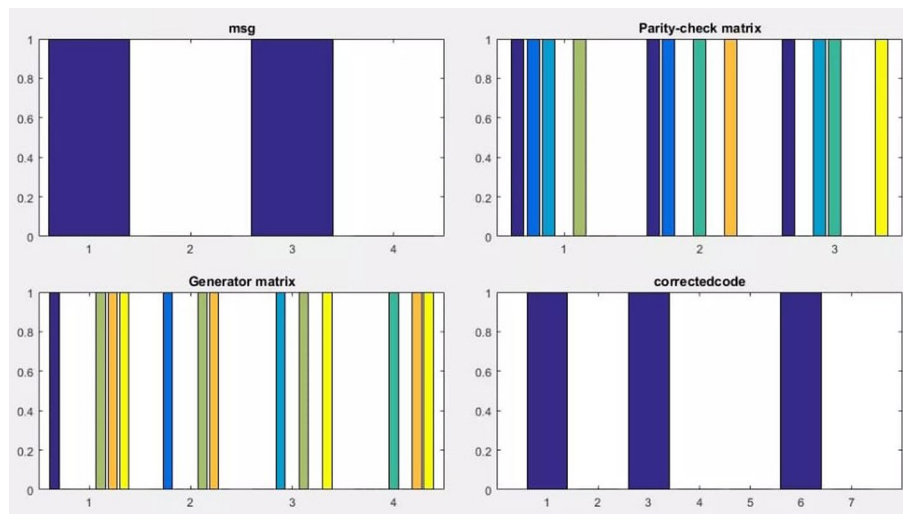

Fig. 3 Performance analysis of Hamming code in MATLAB. In this figure, we have outlined error bits to equality check lattice at that point generator lattice and last adjusted code. To begin with, characterize codeword bits per piece, knead bits per piece, equality sub-matrix, generator lattice, and parity-check network. Encode the message and discover the position of the blunder in the code word (list). At that point, the code alters and adjusts the code. After all, evacuate blunder information at that point plot this figure
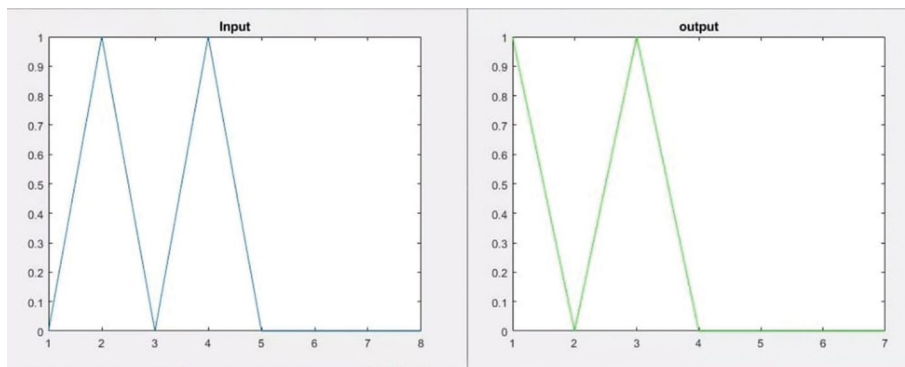
Fig. 4 Performance analysis of Cyclic Redundancy Check in Matlab. In this figure, we have planned input and yield messages with the assistance of CRC. To begin with, we take the input and generate the network. At that point, we discover checksum values. After discovering the checksum, we include a checksum to message bits; at that point, we check yield if the update is nonzero, a transmission mistake has happened, and if the update is zero, no blunders happen, no blunders happen. At that point, the plot yield figure
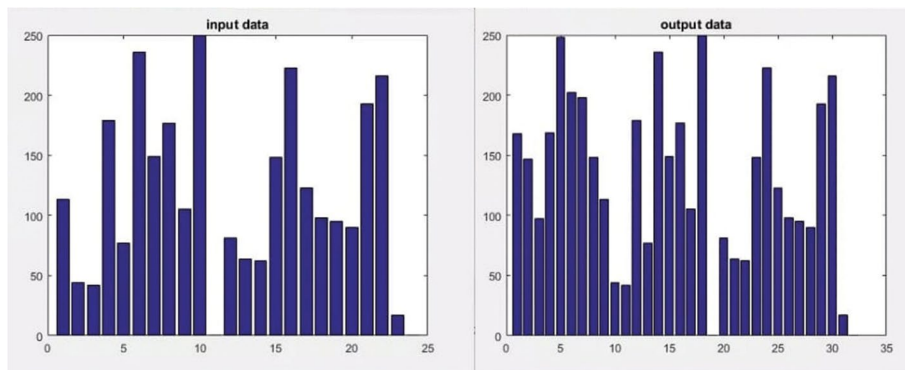
Fig. 5 Performance analysis of Reed Solomon Code in Matlab. In this figure, we have outlined Reed Solomon code as input and yield messages. Reed Solomon code is utilized to adjust burst blunders related. This code is characterized by three parameters a letter set estimate t, square length excite n, and message length k. Decoder characterizes this area utilizing Reed Solomon's code see of codeword as polynomial esteem is based on the message encoded. The decoder recovers the encoding polynomial from the gotten message information in figure

4.4 Performance analysis of EDAC structure

In this Fig. 3, we have outlined error bits to equality check lattice at that point generator lattice and last adjusted code. To begin with, characterize codeword bits per piece, knead bits per piece, equality sub-matrix, generator lattice, and parity-check network. Encode the message and discover the position of the blunder in the code word (list). At that point, the code alters and adjusts the code. After all, evacuate blunder information at that point plot this Fig. 3.

In this Fig. 4, we have planned input and yield messages with the assistance of CRC. To begin with, we take the input and generate the network. At that point, we discover checksum values. After discovering the checksum, we include a checksum to message bits; at that point, we check yield if the update is nonzero, a transmission mistake has happened, and if the update is zero, no blunders happen, no blunders happen. At that point, the plot yield Fig. 4.

Islam *et al. J Wireless Com Network*   (2023) 2023:49

Page 8 of 23

In this Fig. 5, we have outlined Reed Solomon code as input and yield messages. Reed Solomon code is utilized to adjust burst blunders related. This code is characterized by three parameters a letter set estimate *t*, square length excite *n*, and message length *k*. Decoder characterizes this area utilizing Reed Solomon's code see of codeword as polynomial esteem is based on the message encoded. The decoder recovers the encoding polynomial from the gotten message information in Fig. 5.

5   EDAC mechanism V-1.2

5.1 Turbo encoding mechanism

The turbo encoder block uses a parallel concatenated coding scheme to encode a binary input signal [22]. Three identical convolution encoders and two internal interleavers are used in this coding scheme Fig. 6. An interleaver is used between systematic convolution encoders, as In Fig. 6. Here, we can hit a rate of 1/3, without puncturing and 1/2, with a form of puncturing [23]. The process of puncturing also obtains other code rates.
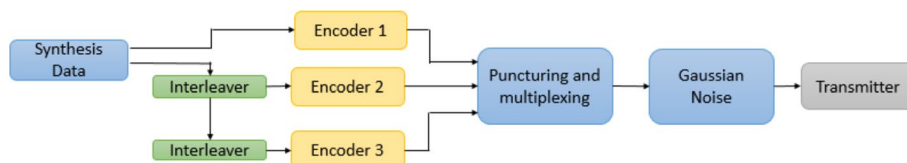

Fig. 6 Advance Turbo Encoder mechanism for EDAC. The turbo encoder block uses a parallel concatenated coding scheme to encode a binary input signal. Three identical convolution encoders and two internal interleavers are used in this coding scheme shown in figure. An interleaver is used between systematic convolution encoders. Here, we can hit a rate of 1/3, without puncturing and 1/2, with a form of puncturing. The process of puncturing also obtains other code rates
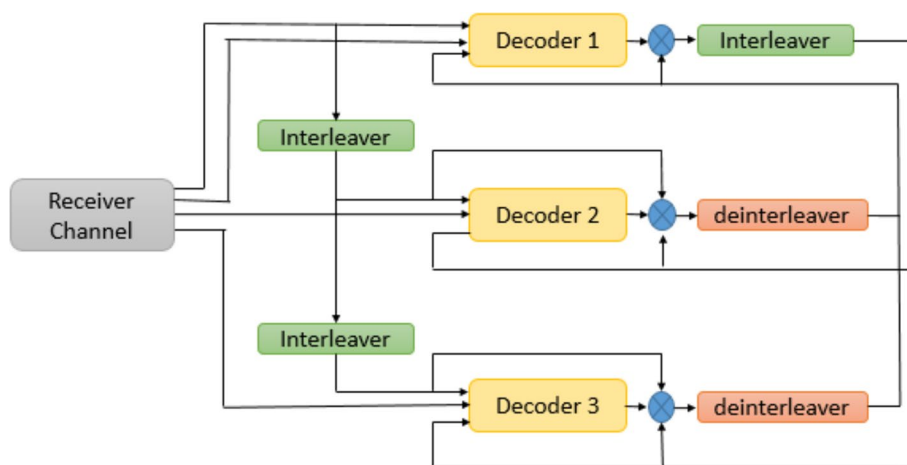

Fig. 7 Advance Turbo Decoder mechanism for EDAC. A turbo decoder is applied when turbo-encoded data is applied to transmission over the AWGN channel via base-band. The Log-Map decoding structure offers less complex output than the limit of Shannon with less complexity. The turbo decoder consists of interleaver and de-interleaver separated SISO decoders, as shown in figure

5.2 Turbo decoding mechanism

A turbo decoder is applied when turbo-encoded data is applied to transmission over the AWGN channel via base-band. The Log-Map decoding structure offers less complex output than the limit of Shannon with less complexity. The turbo decoder consists of interleaver and de-interleaver separated SISO decoders, as shown in Fig. 7.

5.3 Performance analysis of advance turbo mechanism

Turbo codes are better performance codes that result from the interaction of information between recursive codes and decoders of the constitution in Fig. 8.

Turbo code simulated for Rayleigh faded channel for frame size $K=40$. Each SNR's frame number is 500 to keep the simulation fast.

5.4 Additive white Gaussian noise channel (AWGN)

The AWGN channel is one of the most commonly utilized channels that are demonstrated by large used to show an environment with an exceptionally vast number of added substance noise sources. Most added substance commotion sources in modern electronics are a coordinate result of zero-mean warm noise caused by random electron movement inside the resistors, wires, and other components. The AWGN channel may be a well-known model to demonstrate the line of location (LOS) conditions.

5.5 Rayleigh channel

The Rayleigh blurring model is in a perfect world suited to circumstances with vast numbers of flag ways and reflections [24]. Common scenarios consolidate cellular broadcast communications where there's a vast number of reflections from buildings and the like, conjointly HF ionospheric communications where the uneven nature of the ionosphere suggests that, in general, hail can arrive, having taken various assorted ways. This proposition uses a moderate-level independent Rayleigh blurring channel demonstration for the blurring environment [25]. An autonomous Rayleigh blurring handle can be modeled as a steady irregular variable amid each image interim.
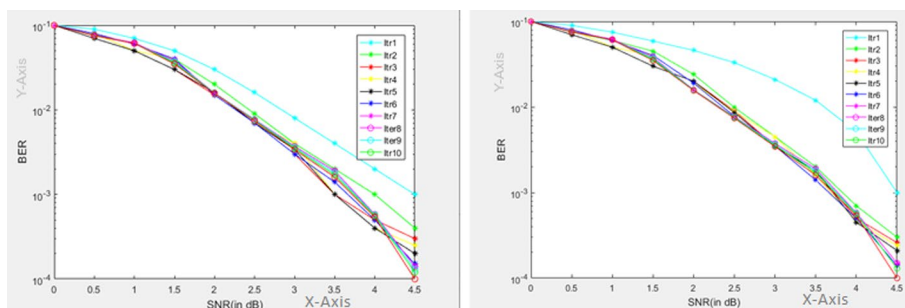

Fig. 8 Performance analysis of turbo code AWGN Channel and Rayleigh Channel. Turbo codes are better performance codes that result from the interaction of information between recursive codes and decoders of the constitution in figure. Turbo code simulated for Rayleigh faded channel for frame size $K=40$. Each SNR's frame number is 500 to keep the simulation fast

6 EDAC Mechanism V-1.3

Five Identical EDAC algorithms are used as encoders LDPC, BCH, Turbo, Convolutional, and Shannon's, and for all the algorithms, random interleavers are used in this coding scheme. Each constituent encoder is terminated by tail bits autonomously. An interleaver is used between five systematic encoders of convolution, as in Fig. 9.

Here, we can hit a rate of 1/3, without puncturing and 1/2, with a form of puncturing. Different EDAC Mechanisms have different bit error rates (BER). If we combine multiple encoding methods in a single one, the BER will be reduced, and the system's performance will be much higher than the single encoding method. We have proposed an architecture that consists of the top 5 EDAC methods for the nanosatellites. Based on communication data EDAC mechanism will be changed. For choosing the coding methods, we used the syntactic machine learning approach. As we know, syntactic analysis finds out the dictionary meaning of any sentence, just like finding the error sequence pattern in a stream of data.
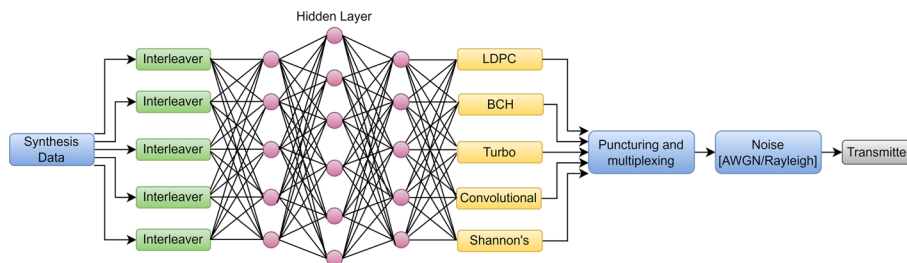

Fig. 9 An Analytical approach to the encoder mechanism for EDAC. Five identical EDAC algorithms are used as encoders LDPC, BCH, Turbo, Convolutional, and Shannon's, and for all the algorithms, random interleavers are used in this coding scheme. Each constituent encoder is terminated by tail bits autonomously. An interleaver is used between five systematic encoders of convolution, as in figure
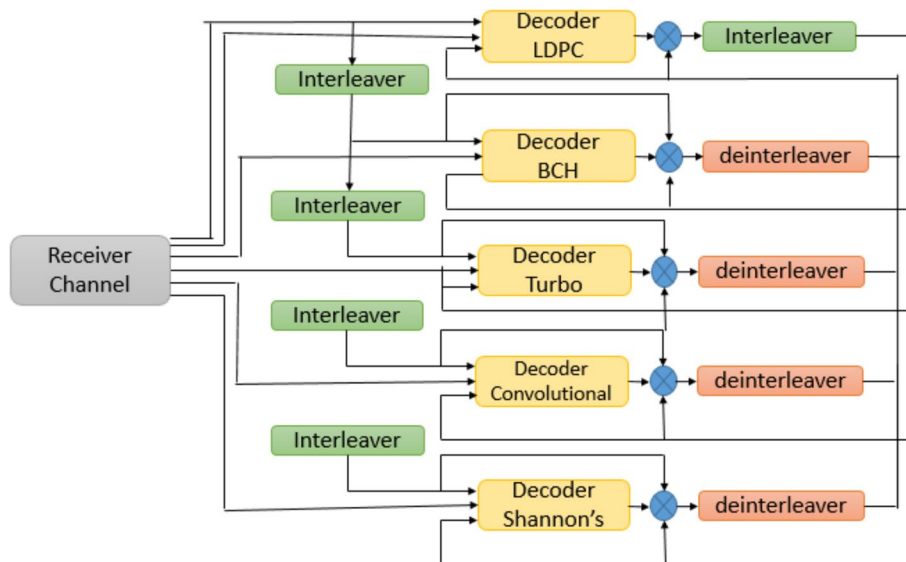

Fig. 10 An Analytical approach to the decoder mechanism for EDAC. Decoder consists of Five interleavers and de-interleavers separated SISO decoders, as shown in Fig. 10. Because of noise, encoded output data bit can get corrupted and enter the input of the decoder as $r0$ for the device bit, $r1$ for parity-1, $r2$ for parity-2, $r3$ for parity-3, $r4$ for parity-4, $r5$ for parity-5. They are fed to the first SISO decoder with these inputs. SISO first, the decoder takes the obtained data bits as input, sequence $r0$ and parity sequence $r1$ got, which is RSC generated encoder 1, Sequence of output results

The process of puncturing also obtains other code rates. The algorithm for decoding can be designed by either an A Probability posterior method or a method of maximum likelihood.

Decoder consists of five interleavers and de-interleavers separated SISO decoders, as shown in Fig. 10. Because of noise, encoded output data bit can get corrupted and enter the input of the decoder as *r0* for the device bit, *r1* for parity-1, *r2* for parity-2, *r3* for parity-3, *r4* for parity-4, *r5* for parity-5. They are fed to the first SISO decoder with these inputs. SISO first, the decoder takes the obtained data bits as input, sequence *r0* and parity sequence *r1* got, which is RSC generated encoder 1, Sequence of output results.

6.1 Low-density parity check (LDPC)

6.1.1 Low-density parity-check encoder

LDPC code design reversible data transmitted is used to LDPC encoder and decoder. A few design methods will be considered to lower the complexity of LDPC code encoding. The technique is to apply the stair code. The ladder structure can be encoded linearly compared to repetitive *H* decoders. Only a single calculation is required to make the encoder effective by general multiplication. Design circuits perform the aspect of the Tanner graph. The same circuits use the encoding and decoding part. Such functions transfer a lot of promise in a function where the circuit area is limited.

6.1.2 Low-density parity-check decoder

The most effective decoders for LDPC codes can be realized by applying repeat message-passing decoders [26]. LDPC code represents by parity check matrix *H*. Tanner's graph is a graph presentation of LDPC, parity matrix. Tanner graph using defined sets of nodes. First variable nodes refer to a single bit of valid code word *x* with the length of the bits. The second set represents the checking node. Constraint a flexible agreement trust extension decoder transmits the probability between checks nodes and variable nodes. This is data transfer local data using finding solutions to a difficult overall complication with less complexity. However, for this type of application, it is necessary to save all the code words that search for 2*K* code words, which are increasing significantly [27]. Faith Promotion Decoder uses repeat messages to pass checks to search for code word *X* and bit nodes.

6.2 Performance analysis of LDPC

AWGN Channel is considered to perform in the best possible way; the only reason is to reduce the power of the channel [28]. The performance of LDPC on AWGN channel in 11. Performance of LDPC codes 10^3 on AWGN channel at SNR $= 0$ dB and BRR 10^{-1} at the same SNR is not for any higher coding than the original. Rayleigh fading is considered the worst-case scenario as there is no effective way. Due to the functionality of the LDPC codes of the relay channel 12, multiple received signals are due to events such as reflection, scratching, and [29]. For example, a comparison of curves in SNR $= 5$ dB implies that the code is BER 10^3 for coding and not BER 10^{-1} for no coding. Figure 11
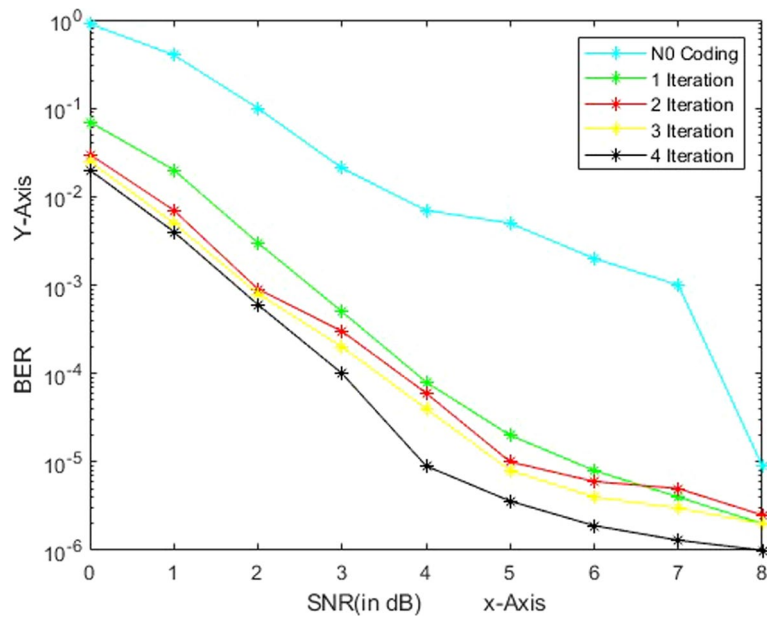
Fig. 11 Performance analysis of LDPC code AWGN Channel. Figures 11 and 12 show the effectiveness of LDPC codes on AWGN, Rayleigh channel. Here the curves are displayed at the same SNR $=2$ dB BER, respectively 10^{-4}, 10^{-1}. The results show that the AWGN channel provides the best performance for the LDPC. It is almost impossible to encounter AWGN channels in real-life applications. In most cases, we have to consider the Rayleigh Fading system that should be built and keep in mind the effects of the Rayleigh channel
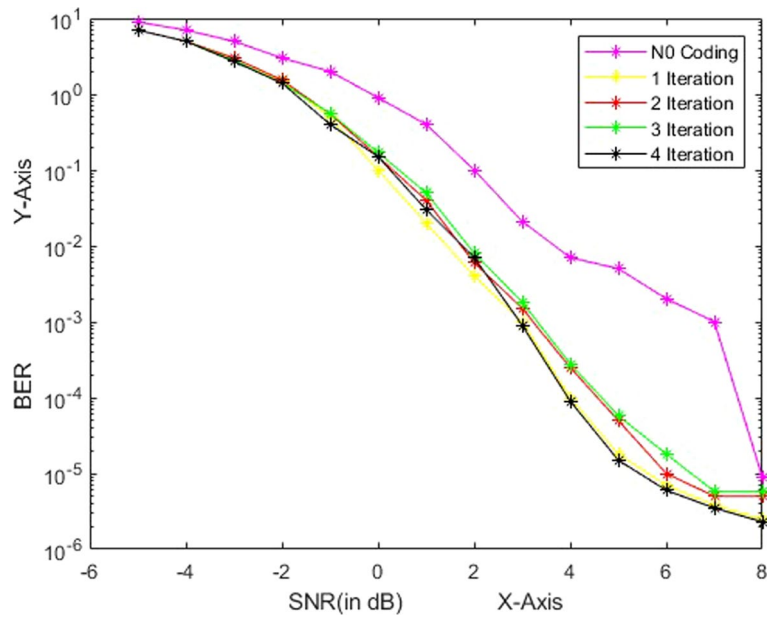

Fig. 12 Performance analysis of LDPC code Rayleigh Channel. Figures 11 and 12 show the effectiveness of LDPC codes on AWGN, Rayleigh channel. Here the curves are displayed at the same SNR $=2$ dB BER, respectively 10^{-4}, 10^{-1}. The results show that the AWGN channel provides the best performance for the LDPC. It is almost impossible to encounter AWGN channels in real-life applications. In most cases, we have to consider the Rayleigh Fading system that should be built and keep in mind the effects of the Rayleigh channel

and 12 show the effectiveness of LDPC codes on AWGN, Rayleigh channel. Here the curves are displayed at the same SNR=2 dB BER, respectively 10^{-4}, 10^{-1}. The results show that the AWGN channel provides the best performance for the LDPC. It is almost impossible to encounter AWGN channels in real-life applications. In most cases, we have to consider the Rayleigh Fading system that should be built and keep in mind the effects of the Rayleigh channel.

6.3 Bose Chaudhuri Hocquenghem (BCH) codes

6.3.1 BCH encoder

Codewords are shaped by including the leftover portion after dividing the message polynomial with the generator polynomial. They are products of the generator polynomial. The generator polynomials are not ordinarily part of the encoding side because they will request more equipment and control circuitry. The polynomial is utilized as such for encoding [30]. The generator polynomial for BCH is given by $1+x^3+x^4+x^5+x^9+x^{12}$ BCH codes are executed as efficient cyclic codes. Consequently, it can be effectively actualized, and the rationale which actualizes the encoder and decoder is controlled into move enrol circuits. The leftover portion can be calculated within the $(n-k)$ straight arrange move registers with the input association at the coefficient of the generator polynomial. LFSR is initialized with seed esteem 0.

6.3.2 BCH decoder

The interpreting handle of the BCH codes comprises three steps. The disorder computation preparation creates *2t* disorders from the gotten code word, which is the data information concatenated with the equality information. At that point, the blunder locator polynomial is computed from the disorders of which the roots point out the blunder positions. Inevitably, the mistakes are adjusted by thoroughly finding out the roots of it utilizing the look calculation. If there is no blunder within the square, we require not one or the other to assess the mistake locator polynomial nor conduct the chain look handle. In this way, to decrease the interpreting time, it is exceptionally important to recognize whether there's any blunder or not as early as conceivable. Here, we propose to check the mistake event with a disorder polynomial by reusing the encoder, which, as it were, requires the GFD, whereas the routine blunder location strategy employments the disorder values, which require a much longer time for conducting a few diverse CGFMs.

6.4 Performance analysis of BCH code

Figure 13 and 14 show the BER plots vs. threshold SNR. For BCH code for two values of average SNR λ_0, 10 dB and 20 dB, with different Doppler frequencies. From the figures, it is clear that an increase in the performance of the BCH code occurs. For large values, the errors tend to be more random as the transition probabilities *b* and *g* increase leading to good performance since the BCH code is capable of correcting such random errors.
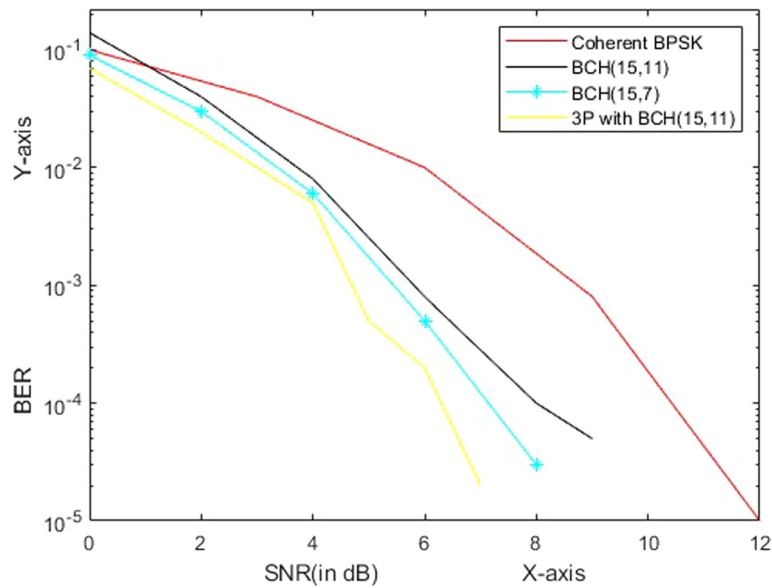
Fig. 13 Performance analysis of BCH code AWGN Channel. Figures 13 and 14 show the BER plots versus threshold SNR. For BCH code for two values of average SNR λ_0, 10 dB and 20 dB, with different Doppler frequencies. From the figures, it is clear that an increase in the performance of the BCH code occurs. For large values, the errors tend to be more random as the transition probabilities b and g increase leading to good performance since the BCH code is capable of correcting such random errors
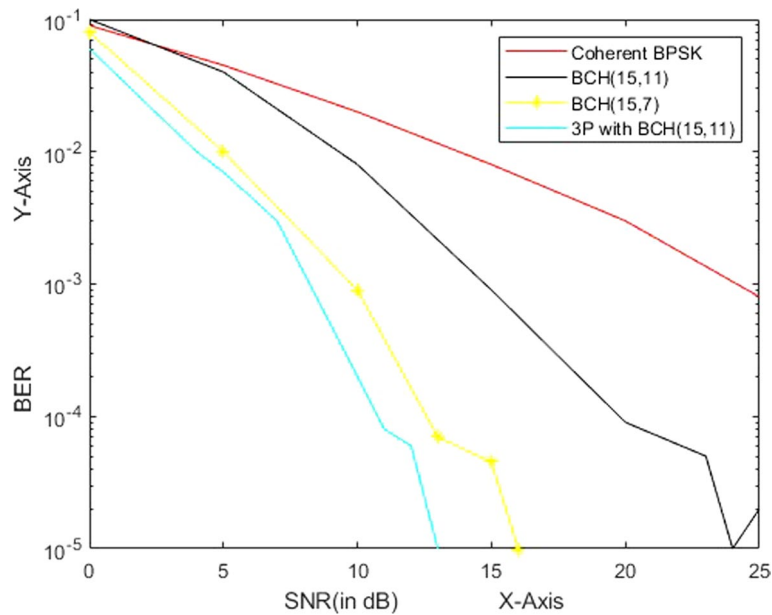

Fig. 14 Performance analysis of BCH code Rayleigh Channel. Figures 13 and 14 show the BER plots versus threshold SNR. For BCH code for two values of average SNR λ_0, 10 dB and 20 dB, with different Doppler frequencies. From the figures, it is clear that an increase in the performance of the BCH code occurs. For large values, the errors tend to be more random as the transition probabilities b and g increase leading to good performance since the BCH code is capable of correcting such random errors
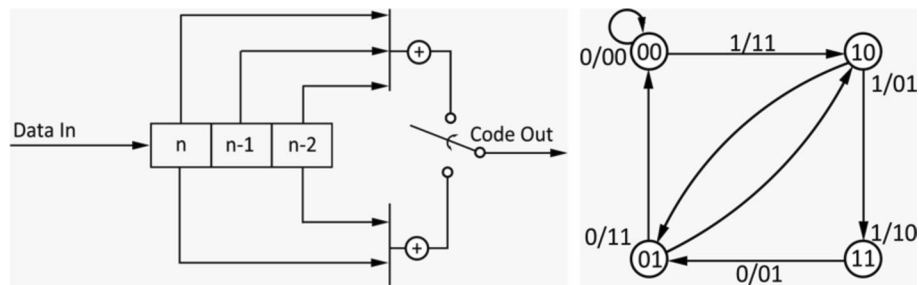
Fig. 15 Convolutional Encoder Systems and State Diagram of Convolutional Code. Inside the encoder, data bits are input to a move enlist of length *K*, called the elemental length. As each bit enters at the cleared out of the select, the past bits are moved to the proper to show disdain toward the truth that the primary orchestrated bit inside the select is evacuated. Two or more twofold summing operations, let's say *r* make code bits that leave inside the center of one data stream period. So, as shown in figure, the code bit rate is *1/r* times the data rate, and the encoder is called a rate *1/r* convolutional encoder of confinement length *K*. It also requires to completely characterize the encoder are the affiliations from stages inside the move select to the *r* summing squares. These generator vectors may be communicated on a very basic level as a push of *K* parallel digits

6.5 Convolutional codes

6.5.1 Convolutional encoder

Inside the encoder, data bits are input to a move enlist of length *K*, called the elemental length. As each bit enters at the cleared out of the select, the past bits are moved to the proper to show disdain toward the truth that the primary orchestrated bit inside the select is evacuated. Two or more twofold summing operations, let's say *r* make code bits that leave inside the center of one data stream period.

In this way Fig. 15, the code bit rate is *1/r* times the data rate, and the encoder is called a rate *1/r* convolutional encoder of confinement length *K*. It also requires to completely characterize the encoder are the affiliations from stages inside the move select to the *r* summing squares. These generator vectors may be communicated on a very basic level as a push of *K* parallel digits.

6.5.2 State diagram

The convolutional encoder shows an outline with $K = 3$, $r = 2$, and the generator vectors are chosen accordingly. Discrete looking at times are labeled *n*. The data stream enters on the cleared out and the show bit at time *n*, the first afterward bit $n - 1$, and the taking after a most reliable bit at $n - 2$ have the move to enlist. Two balance bits are traded out inside the between times between *n* and $n - 1$ from the upper snake and, after that, the lower one. When the taking-after-data bit arrives, the move select moves its substance to the proper. The $K - 1$ earlier bit, in this case, two, choose the state of the encoder. They appeared in gray at 15. In convolutional encoder, there are 2*K* states. For each encoder state, there are two conceivable comes about of yield code bits, depending on whether the input bit is zero or one. At that point, the advancement of states in time can be a work of the information stream. The development of states in time, at that point, may well be a work of the information stream Fig. 15. Each state appears inside a circle, and the alteration from one state to another is shown up by a jar, recognized by the input bit, cut, and yield code bits.
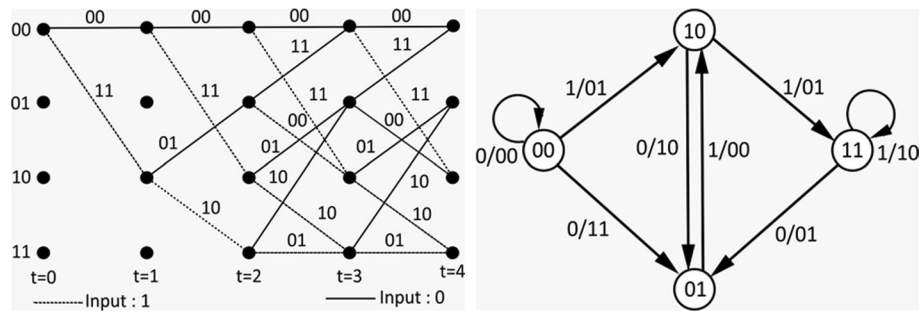
Islam *et al. J Wireless Com Network* (2023) 2023:49

Page 16 of 23

Fig. 16 Trellis structure for a four-state and State diagram of Convolutional Code. Convolutional codes are frequently alluded to as trellis codes due to the reality that trellis charts can effortlessly portray them. The code's trellis chart records the encoder's diverse states and how they are connected. The trellis structure for the state diagram of 16 state diagram appeared in figure. Trellis structure for a four-state encoder. There exist two straightforward approaches to translating a transmitted arrangement of bits. The Viterbi calculation can be utilized by utilizing two primary procedures. The direct approach employs the difficult choice of the received noisy data bits by thresholding the information to parallel digits and applying the calculation. In contrast, the moment approaches employments delicate choice to translate the lead by finding the way among all the ways of the trellis, which has the most significant matrix

6.5.3 Convolutional decoder

Convolutional codes are frequently alluded to as trellis codes due to the reality that trellis charts can effortlessly portray them. The code's trellis chart records the encoder's diverse states and how they are connected. The trellis structure for the state diagram of 16 state diagram appeared in Fig. 16. Trellis structure for a four-state encoder. There exist two straightforward approaches to translating a transmitted arrangement of bits.

The Viterbi calculation can be utilized by utilizing two primary procedures. The direct approach employs the difficult choice of the received noisy data bits by thresholding the information to parallel digits and applying the calculation. In contrast, the moment approaches employments delicate choice to translate the lead by finding the way among all the ways of the trellis, which has the most significant matrix.

6.6 Performance analysis of convolutional code

For the event, at an SNR regard of 5 dB, a bit botch rate of 10^{-5} was gotten. In this regard, 1 bit got in a blunder for 100,000 bits sent. This was far off predominant when the SNR was 2 dB with a bit bumble rate of 10^{-1}. That's 1 bit gotten in botch when 10 bits were sent. For the theoretical BER, the SNR ranges of 2 dB, 2.5 dB, and 3 dB had a bit botch rate of 10^{-1}, whereas, inside the mirrored BER, the SNR was observed to be of the expand 2 dB, 2.5 dB and had the same regard of BER of 10^{-1} whereas the SNR of 3 dB of the imitated BER had an advanced BER of 10^{-2}. This was a result of the convolution coding displayed. Another characteristic was obtained by considering the incline of the hypothetical and imitated regard gotten as in Figs. 17 and 18.

6.7 Shannon's theorem

6.7.1 Shannon's encoding

The included repetition increments the flag's length but permits a more prominent location and adjustment of mistakes amid the translating preparation. Common causes of channel coding incorporate the utilization of equality check bits and redundancy codes.
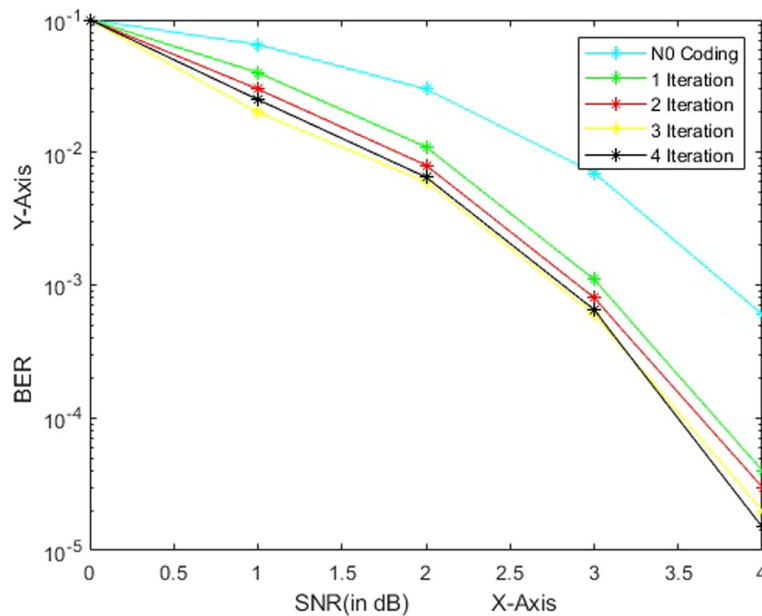
Fig. 17 Performance analysis of Convolutional code AWGN Channel. For the event, at an SNR regard of 5 dB, a bit botch rate of 10^{-5} was gotten. In this regard, 1 bit got in a blunder for 100,000 bits sent. This was far off predominant when the SNR was 2 dB with a bit bumble rate of 10^{-1}. That's 1 bit gotten in botch when 10 bits were sent. For the theoretical BER, the SNR ranges of 2 dB, 2.5 dB, and 3 dB had a bit botch rate of 10^{-1}, whereas, inside the mirrored BER, the SNR was observed to be of the expand 2 dB, 2.5 dB and had the same regard of BER of 10^{-1} whereas the SNR of 3 dB of the imitated BER had an advanced BER of 10^{-2}. This was a result of the convolution coding displayed. Another characteristic was obtained by considering the incline of the hypothetical and imitated regard gotten as in Figs. 17 and 18
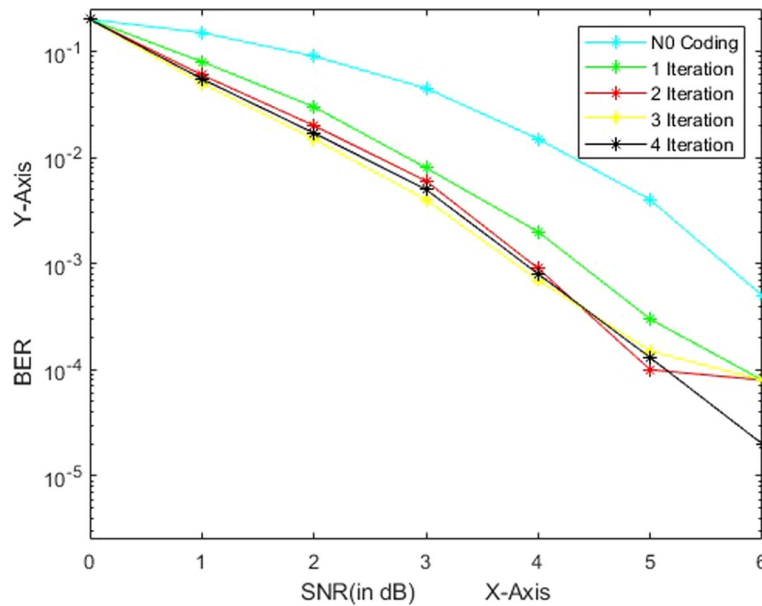

Fig. 18 Performance analysis of Convolutional code Rayleigh Channel. For the event, at an SNR regard of 5 dB, a bit botch rate of 10^{-5} was gotten. In this regard, 1 bit got in a blunder for 100,000 bits sent. This was far off predominant when the SNR was 2 dB with a bit bumble rate of 10^{-1}. That's 1 bit gotten in botch when 10 bits were sent. For the theoretical BER, the SNR ranges of 2 dB, 2.5 dB, and 3 dB had a bit botch rate of 10^{-1}, whereas, inside the mirrored BER, the SNR was observed to be of the expand 2 dB, 2.5 dB and had the same regard of BER of 10^{-1} whereas the SNR of 3 dB of the imitated BER had an advanced BER of 10^{-2}. This was a result of the convolution coding displayed. Another characteristic was obtained by considering the incline of the hypothetical and imitated regard gotten as in Figs. 17 and 18

An equality check bit is essentially an additional bit that's included in a twofold sequence such that there's an indeed number of 1 s. If an arrangement with an odd number of 1's is gotten, at that point, the decoder can identify that a blunder has happened amid transmission through the channel.

6.7.2 Shannon's decoding

The yield of the channel is, at that point, gotten by a decoder, which attempts to change over the gotten flag back to the first message. At that point, at long last, the yield of the decoder is sent to the ultimate client or goal, which is alluded to as the data sink [31]. W speaks to a message. We'll regularly consider that it is the yield of the compressor. The encoder gets W and encodes it to X_n. The encoder puts X_n into the channel, and Y_n is the yield the decoder gets. At long last, the decoder tries to appraise W through Y_n. W_c signifies the decoder's appraisal. Our objective is to get what kind of encodings are such that W_c is the same as W with tall likelihood and n is as little as conceivable.

6.8 Performance evaluation of Shannon's theorem

In Figs. 19 and 20, AWGN Channel and Rayleigh fading, we have used Shannon Theorem. The higher theory is a scale that can be loaded with a BER, with an enabled central signal above the B Hz bandwidth affected by the channel. The term "unfairly BER" means that it has provided conditions for the theorem to be met; in any given BER, no matter how small, we can find the coding process that benefits this BER. The smaller the
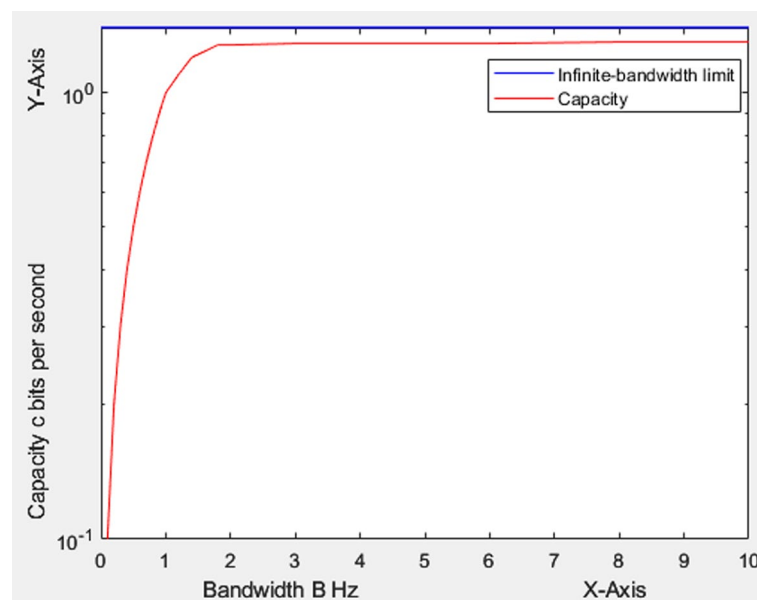

Fig. 19 Performance analysis of Shannon's theorem AWGN Channel. In Figs. 19 and 20, AWGN Channel and Rayleigh fading, we have used Shannon Theorem. The higher theory is a scale that can be loaded with a BER, with an enabled central signal above the B Hz bandwidth affected by the channel. The term "unfairly BER" means that it has provided conditions for the theorem to be met; in any given BER, no matter how small, we can find the coding process that benefits this BER. The smaller the BER given, the harder it will be processed. The least accessible bit rate is called channel capacity C. S/N is a square signal, meaning the sound ratio and logarithm are in base 2

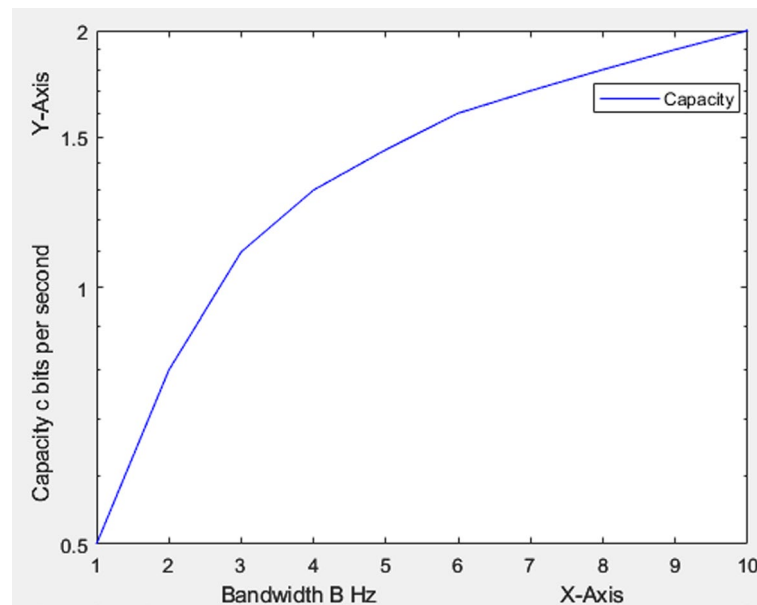Islam *et al. J Wireless Com Network*   (2023) 2023:49

Page 19 of 23

Fig. 20 Performance analysis of Shannon's theorem Rayleigh Channel. In Figs. 19 and 20, AWGN Channel and Rayleigh fading, we have used Shannon Theorem. The higher theory is a scale that can be loaded with a BER, with an enabled central signal above the *B* Hz bandwidth affected by the channel. The term "unfairly BER" means that it has provided conditions for the theorem to be met; in any given BER, no matter how small, we can find the coding process that benefits this BER. The smaller the BER given, the harder it will be processed. The least accessible bit rate is called channel capacity *C*. *S/N* is a square signal, meaning the sound ratio and logarithm are in base 2

BER given, the harder it will be processed. The least accessible bit rate is called channel capacity *C*. *S/N* is a square signal, meaning the sound ratio and logarithm are in base 2.

7 Results and discussion

In analytical Figs. 21 and 22, we apply two types of noise, Rayleigh Channel and AWGN channel, for all algorithms. AWGN Channel is considered to perform in the best possible way and the only reason to reduce the power of the channel. Rayleigh fading is considered the worst-case scenario as there is no effective way. Here, we can see that LDPC, Turbo, Convolutional, BCH, and Shannon's Theorem and these algorithms are best performing for different types of data. Some algorithms are good for less data, and others are better for more data. LDPC works better when signal noise is increasing. Convolutional code works best when signal noise is medium, and the bit error ratio is 10^{-3}.

LDPC works better for the AGWN channel. We transmitted data continuously using machine learning techniques and which type of data was best for which algorithms and identified more error data and removed error data in less time.
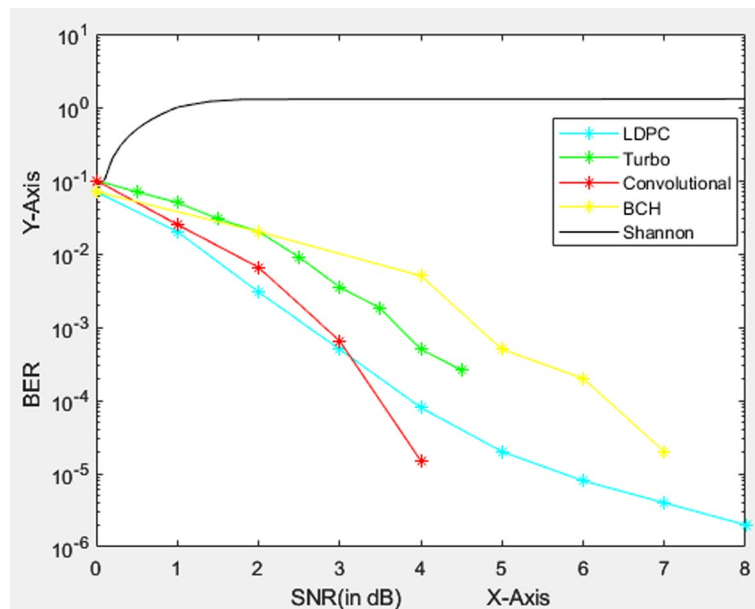
Fig. 21 Performance analysis of hybrid approach for EDAC AWGN Channel. As shown in Figs. 21 and 22, we apply two types of noise, Rayleigh Channel and AWGN channel, for all algorithms. AWGN Channel is considered to perform in the best possible way and the only reason to reduce the power of the channel. Rayleigh fading is considered the worst-case scenario as there is no effective way. Here, we can see that LDPC, Turbo, Convolutional, BCH, and Shannon's Theorem and these algorithms are best performing for different types of data. Some algorithms are good for less data, and others are better for more data. LDPC works better when signal noise is increasing. Convolutional code works best when signal noise is medium, and the bit error ratio is 10^{-3}. LDPC works better for the AGWN channel. We transmitted data continuously using machine learning techniques and which type of data was best for which algorithms and identified more error data and removed error data in less time

8 Limitations and future works

We used multiple algorithms to reduce data transmission error, but these algorithms were limited like an LDPC cannot detect all types of bits errors. LDPC adds extra bits per conversation that have been transmitted through the satellite data transmission system. Turbo code affects single-bit error correction and also detects multiple-bit errors. If numerous-bit error detection is in this code, turbo code can only solve single-bit error correction. A BCH is not suitable for security purposes. BCH is more complex than a checksum and takes more processing. A strong BCH might run slowly in software. But Reed Solomon codes are not efficient as BCH codes. It cannot provide satisfying performance without BCH codes in BPSK modulation schemes.

In the future, we would like to introduce an advanced error detection method based on satellite-transmitted data. Detection algorithms will be changed depending on data size, type, and importance. It might reduce the time of the EDAC process and get reliable, safe data faster. Predicted the less error mechanism in a different type of data. We may use the machine learning technique to find fewer error paths. We implemented the ASIC architecture in Spartan 6 FPGA. After all, we collaborated on our system architecture with Bangabandhu Satellite-1 to have a more secure and faster data transmission.
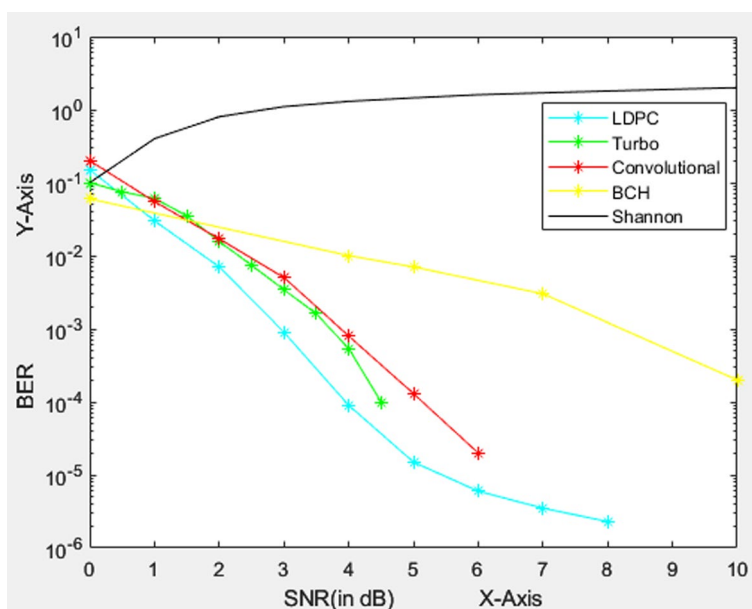
Islam *et al. J Wireless Com Network*   (2023) 2023:49

Page 21 of 23

Fig. 22 Performance analysis of hybrid approach for EDAC Rayleigh Channel. As shown in Figs. 21 and 22, we apply two types of noise, Rayleigh Channel and AWGN channel, for all algorithms. AWGN Channel is considered to perform in the best possible way and the only reason to reduce the power of the channel. Rayleigh fading is considered the worst-case scenario as there is no effective way. Here, we can see that LDPC, Turbo, Convolutional, BCH, and Shannon's Theorem and these algorithms are best performing for different types of data. Some algorithms are good for less data, and others are better for more data. LDPC works better when signal noise is increasing. Convolutional code works best when signal noise is medium, and the bit error ratio is 10^{-3}. LDPC works better for the AGWN channel. We transmitted data continuously using machine learning techniques and which type of data was best for which algorithms and identified more error data and removed error data in less time

9 Conclusions

In this article, we have emphasized different EDAC techniques and code correlation. The proposed approach has attracted the research community. This paper also represents an analytical approach to EDAC algorithms for nanosatellite data transmission systems. Using more complicated error detection and correction codes, the prototype can be expanded for multi-bit errors. The ground station of nanosatellites is continuously maturing and growing impressively. Space technology is continuously evolving and growing in significant ways. All the methods and systems are updated day by day. The automation progress of satellite memory chip architecture is becoming more and more promising, principally with the evolution of nanotechnology.

Abbreviations
EDAC   Error detection and correction
FPGA   Field programmable gate array
AWGN   Additive white Gaussian noise
EO   Earth observation
LDPC   Low density parity check
BCH   Bose Chaudhuri Hocquenghem
LEO   Low earth orbit

Author contributions
All authors contributed to the research conception and design. Data collection was done by MH. Methodology designs were done by MI and MH. Original draft preparation, including review, response and editing, have been done by MI, MH, ZAB. The research has been supervised by MI. All the authors have read and approved the final manuscript.

Availability of data and materials

The data set used and/or analyzed during the current study are available from the corresponding author upon reasonable request.

Declarations

Ethics approval and consent to participate

Not applicable.

Competing interests

The authors declare that they have no competing interests.

References

1. R. Al Mamun, M.M. Islam, R. Tajrin, N. Noor, S. Qader, Error detection and correction for onboard satellite computers using hamming code. Int. J. Electron. Commun. Eng. **14**(9), 251–257 (2020)
2. C. Hillier, V. Balyan, Error detection and correction on-board nanosatellites using hamming codes. J. Electr. Comput. Eng. **2019** (2019)
3. L. You, K.-X. Li, J. Wang, X. Gao, X.-G. Xia, B. Ottersten, Massive mimo transmission for leo satellite communications. IEEE J. Sel. Areas Commun. **38**(8), 1851–1865 (2020)
4. Z. Lin, M. Lin, J.-B. Wang, T. De Cola, J. Wang, Joint beamforming and power allocation for satellite-terrestrial integrated networks with non-orthogonal multiple access. IEEE J. Select. Top. Signal Process. **13**(3), 657–670 (2019)
5. Z. Lin, H. Niu, K. An, Y. Wang, G. Zheng, S. Chatzinotas, Y. Hu, Refracting ris aided hybrid satellite-terrestrial relay networks: joint beamforming design and optimization. IEEE Trans. Aerospace Electr. Syst. (2022)
6. D.E. Friedman, Error control for satellite and hybrid communication networks. PhD thesis, University of Maryland (1995)
7. Z. Lin, K. An, H. Niu, Y. Hu, S. Chatzinotas, G. Zheng, J. Wang, Slnr-based secure energy efficient beamforming in multibeam satellite systems. IEEE Trans. Aerosp. Electr. Syst. (2022)
8. W. Pakartipangi, D. Darlis, B. Syihabuddin, H. Wijanto, A.D. Prasetyo, in *Analysis of camera array on board data handling using fpga for nano-satellite application*, 2015 9th International Conference on Telecommunication Systems Services and Applications (TSSA) (IEEE, 2015), pp. 1–6
9. A. Hanafi, M. Karim, I. Latachi, T. Rachidi, S. Dahbi, S. Zouggar, in *Fpga-based secondary on-board computer system for low-earth-orbit nano-satellite*, 2017 International Conference on Advanced Technologies for Signal and Image Processing (ATSIP) (IEEE, 2017), pp. 1–6
10. M.M. Ibrahim, K. Asami, M. Cho, in *Reconfigurable fault tolerant avionics system*, 2013 IEEE Aerospace Conference (IEEE, 2013), pp. 1–12
11. J.A.P. Celis, S. de la Rosa Nieves, C.R. Fuentes, S.D.S. Gutierrez, A. Saenz-Otero, in *Methodology for designing highly reliable fault tolerance space systems based on cots devices*, 2013 IEEE International Systems Conference (SysCon) (IEEE, 2013), pp. 591–594
12. A.D. George, C.M. Wilson, Onboard processing with hybrid and reconfigurable computing on small satellites. Proc. IEEE **106**(3), 458–470 (2018)
13. R. Banu, T. Vladimirova, in *On-board encryption in earth observation small satellites*, Proceedings 40th Annual 2006 International Carnahan Conference on Security Technology (2006), pp. 203–208
14. R. Banu, T. Vladimirova, Fault-tolerant encryption for space applications. IEEE Trans. Aerosp. Electron. Syst. **45**(1), 266–279 (2009)
15. Y. Bentoutou, A real time edac system for applications onboard earth observation small satellites. IEEE Trans. Aerosp. Electron. Syst. **48**(1), 648–657 (2012)
16. B. Wang, Q. Zhang, in *Study of performance comparison of satellite error correction codes for correcting big burst data errors,* 2018 IEEE 3rd International Conference on Big Data Analysis (ICBDA) (IEEE, 2018), pp. 254–258
17. Gao, N., Xu, Y., He, D., Zhang, G., Zhang, W.: Design of ldpc codes for joint satellite and terrestrial broadcasting system. In: 2018 IEEE International Symposium on Broadband Multimedia Systems and Broadcasting (BMSB), pp. 1–6 (2018). IEEE
18. Y. Liu, Y. Guan, J. Zhang, G. Wang, Y. Zhang, in *Reed-Solomon codes for satellite communications*, 2009 IITA International Conference on Control, Automation and Systems Engineering (case 2009) (IEEE, 2009), pp. 246–249
19. M. Chen, X. Xiao, X. Li, J. Yu, Z.R. Huang, F. Li, L. Chen, Improved ber performance of real-time ddo-ofdm systems using interleaved Reed-Solomon codes. IEEE Photon. Technol. Lett. **28**(9), 1014–1017 (2016)
20. C. Yu, Y.-S. Su, Two-mode Reed-Solomon decoder using a simplified step-by-step algorithm. IEEE Trans. Circuits Syst. II Express Briefs **62**(11), 1093–1097 (2015)
21. E.-H. Lu, T.-C. Chen, P.-Y. Lu, A new method for evaluating error magnitudes of Reed-Solomon codes. IEEE Commun. Lett. **18**(2), 340–343 (2014)
22. S.A. Ali, *Performance analysis of turbo codes over awgn and rayleigh channels using different interleavers*. PhD thesis, Eastern Mediterranean University (2001)

23. Z. Wang, A. Chini, M.T. Kilani, J. Zhou, Multiple-symbol interleaved rs codes and two-pass decoding algorithm. China Commun. **13**(4), 14–19 (2016)
24. D.J. Rhee, S. Rajpal, S. Lin, Some block-and trellis-coded modulations for the rayleigh fading channel. IEEE Trans. Commun. **44**(1), 34–42 (1996)
25. J. Li, A. Bose, Y.Q. Zhao, in *Rayleigh flat fading channels' capacity*, 3rd Annual Communication Networks and Services Research Conference (CNSR'05) (IEEE, 2005), pp. 214–217
26. H. Wang, in *The ldpc code and rateless code for wireless sensor network*, 2019 2nd International Conference on Safety Produce Informatization (IICSPI) (IEEE, 2019), pp. 389–393
27. J. Hou, P.H. Siegel, L.B. Milstein, Performance analysis and code optimization of low density parity-check codes on Rayleigh fading channels. IEEE J. Sel. Areas Commun. **19**(5), 924–934 (2001)
28. X. Pang, C. Yang, Z. Zhang, X. You, C. Zhang, in *A channel-blind decoding for ldpc based on deep learning and dictionary learning,* 2019 IEEE International Workshop on Signal Processing Systems (SiPS) (IEEE, 2019), pp. 284–289
29. D.K. Chy, M. Khaliluzzaman, Evaluation of snr for awgn rayleigh and rician fading channels under dpsk modulation scheme with constant ber. Int. J. Wireless Commun. Mobile Comput. **3**(1), 7–12 (2015)
30. M.Z. Hasan, M.A. Akbar, I. Mahmood, in *Performance analysis of (63, 56) bch code using multipath rayleigh fading channel on spartan-3 fpga*. 2008 2nd International Conference on Advances in Space Technologies (IEEE, 2008), pp. 69–73
31. O. Somekh, S. Shamai, Shannon-theoretic approach to a gaussian cellular multiple-access channel with fading. IEEE Trans. Inf. Theory **46**(4), 1401–1425 (2000)

Publisher's Note

Springer Nature remains neutral with regard to jurisdictional claims in published maps and institutional affiliations.

Md. Motaharul Islam   received a Ph.D. degree from Kyung Hee University, South Korea, in 2013. He is currently working as a Professor in the Dept. of Computer Science and Engineering at United International University. His research interest includes Smart Internet of Things, IP-based Wireless Sensor Networks (IP-WSN), and Cloud Computing.

Mahmudul Hasan   received a B.Sc. degree in Computer Science Engineering from United International University, Dhaka, BangladeshHasan, in 2021. His research interests include Wireless Sensor networks, IoT, Artificial Intelligence, and Machine Learning.

Zaheed Ahmed Bhuiyan   received his master's degree in computer science and engineering from United International University, Bangladesh. He is currently working as a Research Assistant under the supervision of Prof. Md. Motaharul Islam. His major concentration is cybersecurity. His research interests include the Internet of Things (IoT), cloud computing, cloud security, networking, software-defined networking, healthcare technologies, green computing, artificial intelligence, satellite internet communication, and grid-level energy storage systems.